

Stochastic, resonance-free multiple time-step algorithm for molecular dynamics with very large time steps

Ben Leimkuhler,¹ Daniel T. Margul,² and Mark E. Tuckerman³

¹*The Maxwell Institute and School of Mathematics, University of Edinburgh EH9 3JZ, United Kingdom*

²*Department of Chemistry, New York University, New York, NY 10003, USA*

³*Department of Chemistry and Courant Institute of Mathematical Sciences, New York University, New York, NY 10003, USA^a*

(Dated: 17 September 2018)

Molecular dynamics is one of the most commonly used approaches for studying the dynamics and statistical distributions of many physical, chemical, and biological systems using atomistic or coarse-grained models. It is often the case, however, that the interparticle forces drive motion on many time scales, and the efficiency of a calculation is limited by the choice of time step, which must be sufficiently small that the fastest force components are accurately integrated. Multiple time-stepping algorithms partially alleviate this inefficiency by assigning to each time scale an appropriately chosen step-size. However, such approaches are limited by resonance phenomena, wherein motion on the fastest time scales limits the step sizes associated with slower time scales. In atomistic models of biomolecular systems, for example, resonances limit the largest time step to around 5-6 fs. Stochastic processes promote mixing and ergodicity in dynamical systems and reduce the impact of resonant modes. In this paper, we introduce a set of stochastic isokinetic equations of motion that are shown to be rigorously ergodic and that can be integrated using a multiple time-stepping algorithm which is easily implemented in existing molecular dynamics codes. The technique is applied to a simple, illustrative problem and then to a more realistic system, namely, a flexible water model. Using this approach outer time steps as large as 100 fs are shown to be possible.

^a)Electronic mail: mark.tuckerman@nyu.edu

I. INTRODUCTION

Sampling the conformational equilibria of complex systems remains a major challenge in molecular simulation. If achieved, problems such as biomolecular structure prediction, exploration of polymorphism in molecular crystals, and determination of equilibria in glassy systems, to name just a few, would be significantly impacted. Numerous approaches have been developed to accelerate sampling of the Boltzmann distribution, many of which employ molecular dynamics (MD) as the basic engine for driving the exploration of configuration space¹⁻¹⁵. However, methods such as these do not address the underlying inefficiency associated with the inherent broad range of time scales present in the interparticle forces. Multiple time step (MTS) integrators¹⁶⁻²³ were designed to address this problem, and they are capable of improving the efficiency of MD-based approaches even further. However, because MTS methods are essentially perturbative in nature, their efficiency is strongly limited by resonance phenomena^{24,25}, which limit the largest time step to $\Delta t \lesssim 5$ fs for many types of problem, including biomolecular systems treated with an atomistic model. The resonance problem thus poses a major bottleneck for MTS schemes.

Some time ago, Minary *et al.* introduced an MTS algorithm which eliminates (or at least controls) resonance phenomena²⁶. The algorithm is an extended phase-space method based on the Nosé-Hoover chain approach (NHC)²⁷ combined with a set of isokinetic constraints²⁸⁻³¹ that couple the physical degrees of freedom to the NHC thermostats. The isokinetic constraints restrict the energy that can build up in any one mode of motion, thereby moderating the effect of the resonance. The scheme is termed “Iso-NHC-RESPA”, as it starts from the original reference system propagator algorithm (RESPA) introduced by Tuckerman *et al.*¹⁶ and builds in the reversible isokinetic integration algorithms introduced by Zhang²⁹ and by Tuckerman *et al.*³⁰ and the reversible NHC integrators of Martyna *et al.*¹⁹. Using the Iso-NHC-RESPA approach, MD simulations for conformational sampling can be performed with outer time steps as large as 100 fs, and in rigid body MD, even larger outer time steps are possible³². It is important to note, however, that the dynamics are not preserved in the Iso-NHC-RESPA scheme due to the strongly non-Hamiltonian nature of the underlying equations of motion^{33,34} resulting from a large number of isokinetic constraints. More recently, Morrone *et al.* showed that coloured noise thermostats²³ can be used to devise resonant-free MTS algorithms that are able to

preserve the dynamics, although the gains in time step are more modest.

In Ref. 26, it was suggested that each physical degree of freedom be coupled to its own NHC thermostat through an isokinetic constraint in a “massive” thermostating approach. The massive thermostats, as proposed, have two notable limitations

- Since the thermostat is applied to each degree of freedom, the integration of the many NHC thermostats carries an overhead.
- Although in many practical applications NHC methods appear to be ergodic, no proof exists of this fact, hence also the ergodicity of the fully deterministic massive, isokinetic NHC method must be regarded as not established from a mathematical perspective.

Both of these issues can be addressed by introducing a stochastic modification of the equations in place of the thermostating chain³⁵. This has been referred to as the *Nosé-Hoover-Langevin* (NHL) method in Ref. 36, where it was also proved to be ergodic when applied to linear systems.

In this paper, we show that the Iso-NHC-RESPA scheme can be reformulated as a resonant-free MTS algorithm replacing the thermostat chains with the stochastic NHL scheme, thereby allowing an increase in the efficiency of the approach without a reduction in the outer time step. We refer to this method as Stochastic-Iso-NH-RESPA or SIN(R) for short. The “R” for “RESPA” is included parenthetically as a reminder that the SIN(R) scheme can be used purely as a thermostating method without inclusion of RESPA multiple time stepping. However, the real advantage of the method will be demonstrated when it is employed as an MTS approach.

The paper is organized as follows. In Sec. II, we give the equations of motion. We include a formulation incorporating a chain of auxiliary thermostating variables as well as a stochastic perturbation. Sec. III contains an analysis of the properties of the method, including (a) the study of its invariant distribution based on the non-Hamiltonian statistical mechanical formalism (refs. 33 and 34), and (b) a discussion of the ergodicity of method (for a harmonic model problem) using the Hörmander condition. In Sec. IV, we provide the details of a recommended numerical integrator for the equations of motion and discuss its advantages over other possible schemes. In Sec. V, we provide a number of

numerical examples and demonstrate the performance of the method. In this section, we also examine the errors associated with different choices of the parameters. Conclusions are given in Sec. VI.

II. EQUATIONS OF MOTION

Consider a system of N particles in d dimensions with coordinates $q_1, \dots, q_{dN} \equiv q$, momenta $p_1, \dots, p_{dN} \equiv p$, and masses m_1, \dots, m_N . The interparticle forces present between the particles are denoted $F_1(q), \dots, F_{dN}(q)$, and these are assumed to give rise to motion on a wide variety of time scales ranging from fast bond vibrations to slowly varying long-range electrostatic and van der Waals components and are derived from an N -particle potential $U(q_1, \dots, q_{dN}) \equiv U(q)$. Let $\alpha = 1, \dots, dN$, let $v_\alpha = \dot{q}_\alpha$ be the velocity associated with q_α , and let m_α be associated mass. For each coordinate in the system, we introduce the following set of stochastic equations of motion:

$$\begin{aligned}
 dq_\alpha &= v_\alpha dt \\
 dv_\alpha &= \left[\frac{F_\alpha(q)}{m_\alpha} - \lambda_\alpha v_\alpha \right] dt \\
 dv_{1,\alpha} &= -\lambda_\alpha v_{1,\alpha} dt - v_{2,\alpha} v_{1,\alpha} dt \\
 dv_{2,\alpha} &= \frac{G(v_{1,\alpha})}{Q_2} dt - \gamma v_{2,\alpha} dt + \sigma dW_\alpha
 \end{aligned} \tag{1}$$

where $v_{1,\alpha}$ and $v_{2,\alpha}$ are auxiliary thermostat variables, $\sigma = \sqrt{2\gamma/\beta Q_2}$, γ is the friction constant, $\beta = 1/k_B T$, T is the temperature of the system, k_B is Boltzmann's constant,

$$G(v) = Q_1 v^2 - \beta^{-1} \tag{2}$$

Q_1 and Q_2 are thermostat coupling parameters, and λ_α is a Lagrange multiplier for enforcing an isokinetic constraint between the physical velocity v_α and the thermostat velocity $v_{1,\alpha}$ on each degree of freedom:

$$m v_\alpha^2 + \frac{1}{2} Q_1 v_{1,\alpha}^2 = \beta^{-1} \tag{3}$$

As will be seen in Sec. III, this form of the isokinetic constraint ensures that a proper canonical distribution in the coordinates is generated. Note, however, that the individual values of mv_α^2 and $Q_1v_{1,\alpha}^2$ are not what one would expect from a canonical distribution in the velocities but rather correspond to a particular type of microcanonical distribution in each subset $\{v_\alpha, v_{1,\alpha}\}$ of particle velocities³¹. An explicit expression for the Lagrange multiplier can be obtained by differentiating Eq. (3) with respect to time, which yields

$$2mv_\alpha\dot{v}_\alpha + Q_1v_{1,\alpha}\dot{v}_{1,\alpha} = 0, \quad (4)$$

substituting the equations of motion in for \dot{v}_α and $\dot{v}_{1,\alpha}$ to give

$$2mv_\alpha \left[\frac{F_\alpha(q)}{m_\alpha} - \lambda_\alpha v_\alpha \right] + Q_1v_{1,\alpha} [-\lambda_\alpha v_{1,\alpha} - v_{2,\alpha}v_{1,\alpha}] = 0, \quad (5)$$

and then solving for λ_α . The result is

$$\lambda_\alpha = \frac{v_\alpha F_\alpha(q) - \frac{1}{2}Q_1v_{1,\alpha}^2 v_{2,\alpha}}{mv_\alpha^2 + \frac{1}{2}Q_1v_{1,\alpha}^2} \quad (6)$$

The symbol dW_α appearing in Eq. (1) stands for the infinitesimal increment of a Wiener process $W_\alpha(t)$, that is, a “white noise” stochastic process, continuous in t , and such that $W_\alpha(t) - W_\alpha(s)$ is normally distributed with mean zero and variance $|t - s|$, whereas W_i and W_j are independent processes if $i \neq j$. The equations are thus taken to be a system of stochastic differential equations in the Ito sense. The coupling between $v_{1,\alpha}$ and $v_{2,\alpha}$ is of the Nosé-Hoover type with a Langevin-like driving of the variable $v_{2,\alpha}$ (similar to the Nosé-Hoover-Langevin method^{35,36}). If Eq. (6) is substituted into Eqs. (1),

the resulting equations of motion become

$$\begin{aligned}
dq_\alpha &= v_\alpha dt \\
dv_\alpha &= \left[\frac{F_\alpha(q)}{m_\alpha} - \frac{v_\alpha F_\alpha(q) - \frac{1}{2}Q_1 v_{1,\alpha}^2 v_{2,\alpha}}{mv_\alpha^2 + \frac{1}{2}Q_1 v_{1,\alpha}^2} v_\alpha \right] dt \\
dv_{1,\alpha} &= -\frac{v_\alpha F_\alpha(q) - \frac{1}{2}Q_1 v_{1,\alpha}^2 v_{2,\alpha}}{mv_\alpha^2 + \frac{1}{2}Q_1 v_{1,\alpha}^2} v_{1,\alpha} dt - v_{2,\alpha} v_{1,\alpha} dt \\
dv_{2,\alpha} &= \frac{G(v_{1,\alpha})}{Q_2} dt - \gamma v_{2,\alpha} dt + \sigma dW_\alpha
\end{aligned} \tag{7}$$

From Eqs. (7), an important fact about the equations of motion can be derived. In particular, if we use the fact that $Q_1 v_{1,\alpha}^2/2 = \beta^{-1} - mv_\alpha^2$, the equation of motion for $v_{1,\alpha}$ can be expressed as

$$dv_{1,\alpha} = - \left[\frac{v_\alpha F_\alpha(q) - (\beta^{-1} - mv_\alpha^2) - \beta^{-1} v_{2,\alpha}}{\beta^{-1}} \right] v_{1,\alpha} dt \tag{8}$$

which can also be written as

$$d \ln |v_{1,\alpha}| = - \left[\frac{v_\alpha F_\alpha(q) - (\beta^{-1} - mv_\alpha^2) - \beta^{-1} v_{2,\alpha}}{\beta^{-1}} \right] dt \tag{9}$$

The consequence of Eq. (9) is that $v_{1,\alpha}$ can never change sign. Hence, its domain is either $v_{1,\alpha} \geq 0$ or $v_{1,\alpha} \leq 0$.

As was done in Ref. 26, it is possible to generalize Eqs. (1) to incorporate a set of $2L$ thermostat variables, which slightly modifies the form of the equations of motion to read:

$$\begin{aligned}
dq_\alpha &= v_\alpha dt \\
dv_\alpha &= \left[\frac{F_\alpha(q)}{m_\alpha} - \lambda_\alpha v_\alpha \right] dt \\
dv_{1,\alpha}^{(k)} &= -\lambda_\alpha v_{1,\alpha}^{(k)} dt - v_{2,\alpha}^{(k)} v_{1,\alpha}^{(k)} dt \\
dv_{2,\alpha}^{(k)} &= \frac{G(v_{1,\alpha}^{(k)})}{Q_2} dt - \gamma v_{2,\alpha}^{(k)} dt + \sigma dW_\alpha^{(k)}
\end{aligned} \tag{10}$$

with the isokinetic constraint taking the form

$$mv_\alpha^2 + \frac{L}{L+1} \sum_{k=1}^L Q_1 \left(v_{1,\alpha}^{(k)} \right)^2 = L\beta^{-1} \quad (11)$$

Again, the form of this constraint is chosen to give a proper canonical distribution in the coordinates as we will show in Sec. III²⁶. There it will be shown that the distribution generated is a product of microcanonical distributions in the subsets $\{v_\alpha, v_{1,\alpha}^{(k)}\}$ for each degree of freedom. Following the procedure outlined previously of differentiating the constraint once with respect to time and substituting the equations of motion in for the time derivatives, we find that the expression for the Lagrange multiplier generalizes to

$$\lambda_\alpha = \frac{v_\alpha F_\alpha(q) - \frac{L}{L+1} \sum_{k=1}^L Q_1 \left(v_{1,\alpha}^{(k)} \right)^2 v_{2,\alpha}^{(k)}}{mv_\alpha^2 + \frac{L}{L+1} \sum_{k=1}^L Q_1 \left(v_{1,\alpha}^{(k)} \right)^2} \quad (12)$$

Note that Eq. (11) reduces to Eq. (3) when $L = 1$. Moreover, an argument similar to that lead to Eq. (9) can also be made for this more general case, and it leads to the same restriction on the domain of $v_{1,\alpha}^{(k)}$, *i.e.*, $v_{1,\alpha}^{(k)} \geq 0$ or $v_{1,\alpha}^{(k)} \leq 0$. Concerning the thermostat coupling parameters Q_1 and Q_2 , we recommend that these be chosen in a manner similar to the corresponding parameters of Nosé-Hoover chains^{19,27}, *i.e.*, $Q_1 = Q_2 = k_B T \tau^2$, where τ is a time scale of relevance in the system. However, as we will see in Sec. V, the ability of Eqs. (1) or (10) to produce a canonical configurational distribution is not particularly sensitive to this choice.

III. ANALYSIS OF THE EXTENDED ISOKINETIC SYSTEM

In this section, we discuss Eqns. (11), showing that they generate a canonical distribution in the configuration space of the dN coordinates q_1, \dots, q_{dN} . The analysis proceeds in two stages: first, the demonstration that the method preserves the isokinetic partition function, and second that it is ergodic. The proof of ergodicity is only supplied here for $L = 1$. Extending the proof of ergodicity to arbitrary L would be possible but technically involved, and the property is unlikely to fail as the $L > 1$ case only increases the interaction of the variables compared to $L = 1$.

A. Preservation of the isokinetic distribution

Here we employ a procedure derived by Tuckerman *et al.*^{33,34}. In this scheme, if a set of dynamical equations $\dot{\mathbf{x}} = \xi(\mathbf{x})$, where \mathbf{x} is the full phase-space vector (including any extended phase-space variables) and $\xi(\mathbf{x})$ is a vector field, has N_c conservation laws of the form $\Lambda_l(\mathbf{x}) = C_l$, $l = 1, \dots, N_c$, then, assuming the motion is ergodic, the equations of motion generate a generalized microcanonical distribution for which the corresponding partition function takes the form

$$\Omega(C_1, \dots, C_{N_c}) = \int d\mathbf{x} \sqrt{g(\mathbf{x})} \prod_{l=1}^{N_c} \delta(\Lambda_l(\mathbf{x}) - C_l) \quad (13)$$

Here, $\sqrt{g(\mathbf{x})}d\mathbf{x}$ is a conserved volume element, and $\sqrt{g(\mathbf{x})}$ is a metric factor determined by the compressibility of the equations of motion, which is given by

$$\kappa = \nabla_{\mathbf{x}} \cdot \xi(\mathbf{x}) \quad (14)$$

An explicit form for the equations of motion can be obtained by substituting Eq. (12) into Eqs. (10), which yields

$$\begin{aligned} dq_\alpha &= v_\alpha dt \\ dv_\alpha &= \frac{F_\alpha(q)}{m_\alpha} dt - \left[\frac{v_\alpha F_\alpha(q) - \frac{L}{L+1} \sum_{k=1}^L Q_1 \left(v_{1,\alpha}^{(k)} \right)^2 v_{2,\alpha}^{(k)}}{m v_\alpha^2 + \frac{L}{L+1} \sum_{k=1}^L Q_1 \left(v_{1,\alpha}^{(k)} \right)^2} \right] v_\alpha dt \\ dv_{1,\alpha}^{(k)} &= - \left[\frac{v_\alpha F_\alpha(q) - \frac{L}{L+1} \sum_{j=1}^L Q_1 \left(v_{1,\alpha}^{(j)} \right)^2 v_{2,\alpha}^{(j)}}{m v_\alpha^2 + \frac{L}{L+1} \sum_{j=1}^L Q_1 \left(v_{1,\alpha}^{(j)} \right)^2} \right] v_{1,\alpha}^{(k)} dt - v_{2,\alpha}^{(k)} v_{1,\alpha}^{(k)} dt \\ dv_{2,\alpha}^{(k)} &= \frac{G(v_{1,\alpha}^{(k)})}{Q_2} dt - \gamma v_{2,\alpha}^{(k)} dt + \sigma dW^{(k)} \end{aligned} \quad (15)$$

The next step is the calculation of the phase-space compressibility. For this analysis, we first remove the friction and random force terms from the $v_{2,\alpha}^{(k)}$ equation (we return to this point below).

The compressibility is given by

$$\kappa = \sum_{\alpha=1}^{3N} \left[\frac{\partial \dot{q}_\alpha}{\partial q_\alpha} + \frac{\partial \dot{v}_\alpha}{\partial v_\alpha} + \sum_{k=1}^L \left(\frac{\partial \dot{v}_{1,\alpha}^{(k)}}{\partial v_{1,\alpha}^{(k)}} + \frac{\partial \dot{v}_{2,\alpha}^{(k)}}{\partial v_{2,\alpha}^{(k)}} \right) \right] \quad (16)$$

The equations of motion we will use in the calculation of the compressibility are simply Eqs. (15) with the friction and random force terms removed, which are

$$\begin{aligned} \dot{q}_\alpha &= v_\alpha \\ \dot{v}_\alpha &= \frac{F_\alpha(q)}{m_\alpha} - \left[\frac{v_\alpha F_\alpha(q) - \frac{L}{L+1} \sum_{k=1}^L Q_1 \left(v_{1,\alpha}^{(k)} \right)^2 v_{2,\alpha}^{(k)}}{m v_\alpha^2 + \frac{L}{L+1} \sum_{k=1}^L Q_1 \left(v_{1,\alpha}^{(k)} \right)^2} \right] v_\alpha \\ \dot{v}_{1,\alpha}^{(k)} &= - \left[\frac{v_\alpha F_\alpha(q) - \frac{L}{L+1} \sum_{j=1}^L Q_1 \left(v_{1,\alpha}^{(j)} \right)^2 v_{2,\alpha}^{(j)}}{m v_\alpha^2 + \frac{L}{L+1} \sum_{j=1}^L Q_1 \left(v_{1,\alpha}^{(j)} \right)^2} \right] v_{1,\alpha}^{(k)} - v_{2,\alpha}^{(k)} v_{1,\alpha}^{(k)} \\ \dot{v}_{2,\alpha}^{(k)} &= \frac{G(v_{1,\alpha}^{(k)})}{Q_2}. \end{aligned}$$

These equations possess dN conservation laws of the form

$$\Lambda_\alpha = m v_\alpha^2 + \frac{L}{L+1} \sum_{k=1}^L Q_1 \left(v_{1,\alpha}^{(k)} \right)^2 = L \beta^{-1}. \quad (17)$$

For the purposes of this analysis, we take $m_\alpha = 1$ and $Q_1 = Q_2 = 1$. After some straightforward but tedious algebra, the compressibility can be shown to be

$$\kappa = \sum_{\alpha=1}^{3N} \left[\frac{L}{\Lambda_\alpha} \left(-F_\alpha(q) v_\alpha + \sum_{k=1}^L v_{2,\alpha}^{(k)} \left(v_{1,\alpha}^{(k)} \right)^2 \right) - \sum_{k=1}^L v_{2,\alpha}^{(k)} \right]. \quad (18)$$

Using the fact that $\Lambda_\alpha = L/\beta$, the compressibility can be expressed as a total time derivative

$$\kappa = \beta \left[\frac{dU}{dt} + \frac{d}{dt} \frac{1}{2} \sum_{k=1}^L \left(v_{2,\alpha}^{(k)} \right)^2 \right]. \quad (19)$$

According to Refs. 34, if there exists a function $w(\mathbf{x})$ such that $\kappa(\mathbf{x}) = dw(\mathbf{x})/dt$, then

$$\sqrt{g(\mathbf{x})} = e^{-w(\mathbf{x})}, \quad (20)$$

and the partition function generated by Eqs. (17) is

$$\Omega(N, V, \beta) = \int d^{dN} a d^{dN} p d^{dNL} v_1 d^{dNL} v_2 \rho_{\text{isok}},$$

where

$$\rho_{\text{isok}} = e^{-\frac{\beta}{2} \sum_{k=1}^L (v_{2,\alpha}^{(k)})^2} e^{-\beta U(q)} \times \prod_{\alpha=1}^{dN} \delta \left(v_{\alpha}^2 + \frac{L}{L+1} \sum_{k=1}^L (v_{1,\alpha}^{(k)})^2 - L\beta^{-1} \right), \quad (21)$$

which is clearly canonical in the dN coordinates q_1, \dots, q_{dN} .

Now let us consider effect of the friction and noise terms which we have so far neglected. Note that the invariant distribution generated in $v_{2,\alpha}^{(k)}$ by the Ornstein-Uhlenbeck component is Gaussian. Since the noise process only contacts the $v_{2,\alpha}^{(k)}$ terms, it follows that the remaining part of the distribution function will be left invariant by the action of the corresponding Fokker-Planck equation. We may think of the stochastic differential equations as being divided into two parts:

$$d\mathbf{X} = \underbrace{\mathbf{f}(\mathbf{X})dt}_{\text{deterministic}} + \underbrace{\mathbf{\Gamma}\mathbf{X}dt + \mathbf{\Sigma}d\mathbf{W}}_{\text{Ornstein-Uhlenbeck}} \quad (22)$$

where \mathbf{f} corresponds to the deterministic chain system considered above, and $\mathbf{\Gamma}$ and $\mathbf{\Sigma}$ are suitable matrices which describe the Ornstein-Uhlenbeck-type (linear) stochastic differential equations in each of the v_2 components (\mathbf{W} represents a vector of independent Wiener processes, one contacting each $v_{2,\alpha}^{(k)}$ degree of freedom). The corresponding Fokker-Planck operator inherits an additive decomposition

$$\rho_t = -i\mathcal{L}_1^\dagger \rho - i\mathcal{L}_2^\dagger \rho \quad (23)$$

and we have the property that, in the weak (distributional) sense

$$\mathcal{L}_1^\dagger \rho_{\text{isok}} = 0 \tag{24}$$

and

$$\mathcal{L}_2^\dagger \left[e^{-\frac{\beta}{2} \sum_{k=1}^L (v_{2,\alpha}^{(k)})^2} \hat{\rho} \right] = 0, \tag{25}$$

where $\hat{\rho}$ is an arbitrary, normalizable distribution in the other variables in the system (besides $v_{2,\alpha}^{(k)}$). Clearly $(\mathcal{L}_1^\dagger + \mathcal{L}_2^\dagger) \rho_{\text{isok}} = 0$.

It therefore follows that the isokinetic density ρ_{isok} given above will also be preserved under the dynamics of the full system with the stochastic process incorporated. It remains only to show that this is the unique stationary state of the SDE.

B. Ergodicity

In this subsection we sketch a proof of the ergodicity of the isokinetic model in the case of a single stochastic isokinetic thermostat on a single harmonic oscillator, which, in a certain sense, is the most difficult case (there is no internal mechanism present in the deterministic dynamics to promote mixing). It is likely that, with more effort, the proof could be extended to anharmonic potentials. Theories of ergodicity for stochastic differential equations are now well developed^{37–39}. Consider a stochastic differential equation (SDE) on a smooth manifold M of the form

$$d\mathbf{X} = \mathbf{a}(\mathbf{X})dt + \sum_{i=1}^m \mathbf{b}_i(\mathbf{X})dW_i \tag{26}$$

where dW_i , $i = 1, \dots, m$ are the infinitesimal increments of m independent Wiener processes, and $\mathbf{a}(\mathbf{X})$ and $\mathbf{b}_i(\mathbf{X})$, $i = 1, \dots, m$ are smooth vector fields on the tangent space $TM_{\mathbf{X}}$. Note that Equation 22 can be put in this form by defining $\mathbf{a}(\mathbf{X}) := \mathbf{f}(\mathbf{X}) - \Gamma\mathbf{X}$ and $\sum_{i=1}^m \mathbf{b}_i(\mathbf{X})dW_i \equiv \Gamma d\mathbf{W}$. As mentioned in the previous subsection, corresponding to the SDE there is a Fokker-Planck equation of the form

$$\rho_t = -i\mathcal{L}^\dagger \rho, \tag{27}$$

where $i\mathcal{L}$ is the generator of the stochastic process and $-i\mathcal{L}^\dagger$ is its adjoint. The system is ergodic, implying the convergence of averages along almost every trajectory, provided the solution of $\mathcal{L}^\dagger\rho = 0$ is unique (up to a constant scaling) and $C^\infty(M)$. In the case at hand, we have a smooth stationary distribution (see the previous section) and all that remains is to check that it is unique. We omit some details here (see refs. 36 and 40 for related studies) noting only that the crucial step needed to establish the regularity of the operator (and thus the uniqueness of the invariant density and hence the ergodicity of the stochastic differential equations) is to verify a certain Hörmander condition. The Hörmander condition guarantees that the solutions of $\mathcal{L}^\dagger\rho = 0$ are smooth (in C^∞) and unique.

Let $\mathcal{I}(\mathbf{b}_0 := \mathbf{a}, \mathbf{b}_1, \dots, \mathbf{b}_m)$ denote the ideal generated by $\mathbf{b}_0, \dots, \mathbf{b}_m$:

$$\mathcal{I}(\mathbf{b}_0, \mathbf{b}_1, \dots, \mathbf{b}_m) = \{\mathbf{b}_{k_0}, [\mathbf{b}_{k_0}, \mathbf{b}_{k_1}], [\mathbf{b}_{k_0}, [\mathbf{b}_{k_1}, \mathbf{b}_{k_2}]], \dots\},$$

where $[\cdot, \cdot]$ denotes the commutator of vector fields, k_0, k_1, k_2, \dots , take values in the set $\{0, \dots, m\}$.

The Hörmander condition⁴¹ to ensure a smooth invariant probability measure for this system is

$$TM = \text{span } \mathcal{I}(\mathbf{b}_0, \mathbf{b}_1, \dots, \mathbf{b}_m), \quad (28)$$

Intuitively, the Hörmander condition implies that at any point of our phase space, the dynamics will explore all possible directions, so noise, introduced in one component, filters into all directions. Note that the condition is sometimes stated in a restricted form^{38,39} which does not allow k_0 to have value 0. It is more difficult in many cases to verify this restricted Hörmander condition, the consequence of which is the smoothness of solutions to the time-dependent Fokker-Planck equation for arbitrary nonzero time t . We are interested in the long-term behavior of solutions, i.e. the time-invariant solution of the stationary Fokker-Planck equation, and for this to hold, one may use the simpler Hörmander condition given above. Another technicality that should be addressed is the treatment of an unbounded space; we should consider the contractivity of the flow by constructing a Lyapunov function, as in ref. 40, however, with periodic boundary conditions the configuration space is bounded, and with the isokinetic constraint the velocities

(momenta) and auxiliary variables $v_{1,\alpha}$ remain bounded. All that is left to is to insure that there is no divergence in the $v_{2,\alpha}$ directions, but this is easily shown as they are controlled directly by Wiener (friction+noise) processes.

For a single harmonic oscillator with $L = 1$, the isokinetic stochastic dynamics take the form

$$\begin{aligned}
dq &= v dt \\
dv &= [-q - \lambda v] dt \\
dv_1 &= [-\lambda v_1 - v_2 v_1] dt \\
dv_2 &= [Q^{-1}[v_1^2 - k_B T] - \gamma v_2] dt + \sqrt{2\gamma k_B T/Q} dW
\end{aligned} \tag{29}$$

where

$$\lambda = \frac{-qv - v_2 v_1^2/2}{v^2 + v_1^2/2} \tag{30}$$

The dimension of the extended phase space of this model is three. (There are 4 variables and one constraint, $v^2 + v_1^2/2 = \text{const}$, which defines a 3-dimensional manifold M .)

Note that $v_1 = 0$ is an invariant manifold of the isokinetic equations; the solutions are confined for all time to one or the other half-space ($v_1 < 0$ or $v_1 > 0$). Furthermore observe that the equations of motion for q, v, v_2 all depend on v_1^2 only, thus there is a symmetry between the two domains $v_1 < 0$ and $v_1 > 0$. This symmetry also carries over to the integrand of the extended partition implying that one need only sample one or the other of the two half-spaces.

In order for the system to be ergodic, we must that verify the Hörmander condition holds. For our system, \mathbf{a} and \mathbf{b} are the vector fields

$$\mathbf{a} = v\partial_q - (q + \lambda v)\partial_v - (\lambda v_1 + v_2 v_1)\partial_{v_1} + [Q^{-1}(v_1^2 - k_B T) - \gamma v_2]\partial_{v_2}, \tag{31}$$

and

$$\mathbf{b} = \sigma\partial_{v_2} \tag{32}$$

where $\sigma = \sqrt{2\gamma k_B T/Q}$.

The Hörmander condition we require is this: at any point, the dimension of the ideal

spanned by the iterated commutators of the vector fields \mathbf{a} and \mathbf{b} ,

$$\mathbf{a}, \mathbf{b}, [\mathbf{a}, \mathbf{b}], [\mathbf{a}, [\mathbf{a}, \mathbf{b}]], [\mathbf{b}, [\mathbf{a}, \mathbf{b}]], \dots$$

has dimension 3, that is, it spans the tangent space to the manifold M . We will compute a particular selection from the commutators and show that they form a basis, specifically, we consider the vectors

$$\mathbf{a}, \mathbf{b}, [\mathbf{a}, \mathbf{b}], [\mathbf{a}, [\mathbf{a}, \mathbf{b}]], [\mathbf{a}, [\mathbf{a}, [\mathbf{a}, \mathbf{b}]]].$$

From these vectors, we will find three linearly independent ones at every point except on a one-dimensional set (the union of two lines). We may assume $v_1 \neq 0$ as mentioned above. The fact that the Hörmander condition fails on a set of dimension 1 (i.e. co-dimension 2 relative to the manifold M) is of no consequence as the low-dimensional set cannot restrict the volume of the region explored by stochastic paths. (The paths easily circumnavigate this obstacle.)

Since \mathbf{b} is a constant multiple of $[0, 0, 0, 1]^T$, then it is clear that \mathbf{a} and \mathbf{b} are linearly independent as long as one of the first three components of \mathbf{a} is nonzero. Having all these zero implies $q = 0, v = 0$, in which case v_1 is fixed by the isokinetic constraint, which defines two lines of degenerate points given by $q = 0, v = 0, v_1 = \pm\sqrt{3k_B T}$, with v_2 arbitrary; denote the union of these two lines by M_0 .

Now the commutator \mathbf{a} and \mathbf{b} is given by

$$\begin{aligned} [\mathbf{a}, \mathbf{b}] &= (\sigma v \frac{\partial \lambda}{\partial v_2}) \partial_v + \sigma v_1 \left(1 + \frac{\partial \lambda}{\partial v_2} \right) \partial_{v_1} + \sigma \gamma \partial_{v_2} \\ &= \sigma v \frac{\partial \lambda}{\partial v_2} \partial_v + v_1 \left(1 + \frac{\partial \lambda}{\partial v_2} \right) \partial_{v_1} + \sigma \gamma \partial_{v_2} \end{aligned} \quad (33)$$

Since $\mathbf{b} = \sigma \mathbf{e}_4$, we only need to show that, except possibly on M_0 , the vectors defined by the first three components of \mathbf{a} and $[\mathbf{a}, \mathbf{b}]$ are linearly independent. These are

$$\mathbf{u}_1 = v \partial_q - (q + \lambda v) \partial_v - (\lambda v_1 + v_1 v_2) \partial_{v_1}, \quad (34)$$

and

$$\mathbf{u}_2 = \sigma v \frac{\partial \lambda}{\partial v_2} \partial_v + v_1 \left(1 + \frac{\partial \lambda}{\partial v_2} \right) \partial_{v_1}. \quad (35)$$

After expanding the derivatives of λ we have

$$\mathbf{u}_1 = v \partial_q + v_1^2 \left(\frac{-q + vv_2}{D} \right) \partial_v - 2v_1 v \left(\frac{-q + vv_2}{D} \right) \partial_{v_1}, \quad (36)$$

and

$$\mathbf{u}_2 = -\sigma(v_1^2 v / D) \partial_v + (2\sigma v_1 v^2 / D) \partial_{v_1}, \quad (37)$$

where $D = 2v^2 + v_1^2$.

If $q \neq 0$ and $v \neq 0$, then clearly \mathbf{u}_1 and \mathbf{u}_2 are linearly independent. However, if $v = 0$ then $\mathbf{u}_2 = 0$.

For this reason we must compute an additional commutator $[\mathbf{a}, [\mathbf{a}, \mathbf{b}]]$. Projecting to the first three components (since we already have that \mathbf{e}_4 is in our subspace) results in

$$\mathbf{u}_3 = \sigma \left(\frac{v_1^2 v}{D} \right) \partial_q - \sigma \left(\frac{2\gamma v^3 + \gamma v_1^2 v - v_1^2 q}{D^2} \right) \partial_v + 2\sigma v_1 v \left(\frac{2\gamma v^3 + \gamma v_1^2 v - v_1^2 q}{D^2} \right) \partial_{v_1}. \quad (38)$$

Again, we substitute $v = 0$ and find that

$$\mathbf{u}_3|_{v=0} = (\sigma v_1^2 q / D^2) \partial_v. \quad (39)$$

Unfortunately, this is parallel to \mathbf{u}_1 (for $v = 0$), and hence another commutator is required.

Computing $[\mathbf{a}, [\mathbf{a}, [\mathbf{a}, \mathbf{b}]]]$ and projecting to the first three components yields

$$\begin{aligned} \mathbf{u}_4 = & \sigma \left(\frac{2\gamma v^3 - 4v^3 v_2 + 4v^2 q + v_1^2 v v_2 + \gamma v_1^2 v - 2v_1^2 q}{D^2} \right) \partial_q \\ & - \sigma v_1^2 \left(\frac{\eta}{D^3} \right) \partial_v + 2\sigma v_1 v \left(\frac{\eta}{D^3} \right) \partial_{v_1}. \end{aligned} \quad (40)$$

where

$$\begin{aligned} \eta = & 4v^5 \gamma^2 - 8v^5 Q^{-1} v_1^2 - 4v_1^2 v^3 + 4v^3 \gamma^2 v_1^2 - 4v^3 v_1^4 Q^{-1} \\ & - 2\gamma v_1^2 v^2 q + 4v^2 q v_2 v_1^2 - 4v_1^2 q^2 v - 2v_1^4 v + v \gamma^2 v_1^4 - q \gamma v_1^4 + v_1^4 v_2 q. \end{aligned} \quad (41)$$

Now along $v = 0$ we find that \mathbf{u}_4 simplifies to

$$\begin{aligned}\mathbf{u}_4|_{v=0} &= -2\sigma q \partial_q - \sigma \left(\frac{-q\gamma v_1^4 + v_1^4 v_2 q}{v_1^4} \right) \partial_v \\ &= -2\sigma q \partial_q - \sigma q (-\gamma + v_2) \partial_v\end{aligned}\tag{42}$$

Finally we see that this and \mathbf{u}_1 form a linearly independent set if $q \neq 0$. (Of course if $v = q = 0$ then we are on M_0 .)

Thus we see that, off of the low-dimensional set M_0 , the Hörmander condition is verified for the stochastic isokinetic method applied to the harmonic oscillator. We therefore conclude that the invariant measure of the stochastic isokinetic system (in the case of the harmonic oscillator) is unique, and thus that the process is ergodic.

IV. MULTIPLE TIME STEP INTEGRATION ALGORITHM

In this section, we derive a multiple time-step (MTS) integrator for the equations of motion (11), based on the reference system propagator algorithm (RESPA) introduced by Tuckerman *et al.*¹⁶. In this derivation, in order to simplify the notation, we will drop the α index, which labels the degrees of freedom in the system. However, it must be kept in mind that the integrator obtained should be applied to *each* degree of freedom in the system.

The derivation begins with the Liouville operator for the equations of motion given by

$$iL = iL_q + iL_v + iL_N + iL_{OU}\tag{43}$$

where

$$\begin{aligned}
iL_q &= v \frac{\partial}{\partial q} \\
iL_v &= \left(\frac{F}{m} - \lambda_F v \right) \frac{\partial}{\partial v} - \lambda_F \sum_{k=1}^L v_1^{(k)} \frac{\partial}{\partial v_1^{(k)}} \\
iL_N &= -\lambda_N v \frac{\partial}{\partial v} - \lambda_N \sum_{k=1}^L v_1^{(k)} \frac{\partial}{\partial v_1^{(k)}} - \sum_{k=1}^L v_2^{(k)} v_1^{(k)} \frac{\partial}{\partial v_1^{(k)}} + \sum_{k=1}^L \frac{G(v_1^{(k)})}{Q_2} \frac{\partial}{\partial v_2^{(k)}} \quad (44)
\end{aligned}$$

and iL_{OU} corresponds to the Ornstein-Uhlenbeck-type stochastic process applied to $v_2^{(k)}$. A numerical integrator is derived via an MTS factorization of the classical propagator $\exp(iL\Delta t)$ based on the Trotter theorem, where Δt is a time step appropriate for the slowest motion. In the derivation to follow, we will build on a basic factorization scheme for Langevin dynamics recently studied in depth by Matthews and Leimkuhler⁴², in particular separating and treating exactly the Ornstein-Uhlenbeck term. The multiplier in Eq. (12) contains two contributions, which we express as $\lambda = \lambda_F + \lambda_N$, referring to the contributions from the force F and the Nosé-like coupling to the extended phase-space variables $v_1^{(k)}$. For standard Langevin dynamics, obtained from Eq. (44) by setting $iL_N = 0$ and $\lambda_F = \lambda_N = 0$ so that $iL_v = (F/m)(\partial/\partial v)$, the factorization takes the form

$$e^{iL\Delta t} = e^{iL_v\Delta t/2} e^{iL_q\Delta t/2} e^{iL_{OU}\Delta t} e^{iL_q\Delta t/2} e^{iL_v\Delta t/2} \quad (45)$$

Extending this to the stochastic isokinetic Liouville operator of Eq. (44), the corresponding single time-step integrator would take the form

$$e^{iL\Delta t} = e^{iL_N\Delta t/2} e^{iL_v\Delta t/2} e^{iL_q\Delta t/2} e^{iL_{OU}\Delta t} e^{iL_q\Delta t/2} e^{iL_v\Delta t/2} e^{iL_N\Delta t/2} \quad (46)$$

Eq. (46) could be employed as a starting point for the derivation of a robust numerical scheme by applying it together with the integrators of Refs. 26 and 30.

In order to derive an MTS algorithm, suppose the force contains a fast and a slow

component: $F = F_f + F_s$. With this division, the Liouville operator can be expressed as

$$iL = iL_q + iL_v^{(f)} + iL_v^{(s)} + iL_N + iL_{OU} \quad (47)$$

where the contributions $iL_v^{(f)}$ and $iL_v^{(s)}$ are determined by the fast and slow force components and their contributions to the Lagrange multiplier:

$$\begin{aligned} iL_v^{(f)} &= \left(\frac{F_f}{m} - \lambda_F^{(f)} v \right) \frac{\partial}{\partial v} - \lambda_F^{(f)} \sum_{k=1}^L v_1^{(k)} \frac{\partial}{\partial v_1^{(k)}} \\ iL_v^{(s)} &= \left(\frac{F_s}{m} - \lambda_F^{(s)} v \right) \frac{\partial}{\partial v} - \lambda_F^{(s)} \sum_{k=1}^L v_1^{(k)} \frac{\partial}{\partial v_1^{(k)}} \end{aligned} \quad (48)$$

The corresponding Lagrange multiplier contributions are

$$\begin{aligned} \lambda_F^{(f)} &= \frac{v F_f}{\Lambda} \\ \lambda_F^{(s)} &= \frac{v F_s}{\Lambda} \\ \lambda_N &= -\frac{(L/L + 1) \sum_{j=1}^L Q_1 \left(v_1^{(j)} \right)^2 v_2^{(j)}}{\Lambda} \end{aligned} \quad (49)$$

and $\Lambda = mv^2 + (L/L + 1) \sum_k Q_1 \left(v_1^{(k)} \right)^2 = L\beta^{-1}$.

RESPA integrators for extended-system thermostatted MD equations of motion are of two types described in Ref. 19 depending on the placement of the evolution step of the extended phase-space variables in the algorithm. When these steps are at the beginning and end of the overall integration step, the approach is called an extended-system “outer” RESPA or XO-RESPA scheme. When these steps are carried out with the evolution of the fastest motion, the scheme is called an extended-system inner RESPA or XI-RESPA scheme. These two schemes involve different factorizations of the classical propagator. Let Δt and δt be the time steps associated with the slow and fast force components,

respectively. Then, the proposed XO-RESPA factorization can be written as

$$\begin{aligned}
\exp(iL\Delta t) &= \exp\left(iL_N\frac{\Delta t}{2}\right) \\
&\times \exp\left\{\frac{\delta t}{2}\left[\left(\frac{F_f + nF_s}{m} - (\lambda_F^{(f)} + n\lambda_F^{(s)})\right)\frac{\partial}{\partial v} - (\lambda_F^{(f)} + n\lambda_F^{(s)})\sum_{k=1}^L v_1^{(k)}\frac{\partial}{\partial v_1^{(k)}}\right]\right\} \\
&\times \exp\left(\frac{\delta t}{2}v\frac{\partial}{\partial q}\right)\exp(iL_{OU}\delta t)\exp\left(\frac{\delta t}{2}v\frac{\partial}{\partial q}\right) \\
&\times \exp\left\{\frac{\delta t}{2}\left[\left(\frac{F_f}{m} - \lambda_F^{(f)}\right)\frac{\partial}{\partial v} - \lambda_F^{(f)}\sum_{k=1}^L v_1^{(k)}\frac{\partial}{\partial v_1^{(k)}}\right]\right\} \\
&\times \left[\exp\left\{\frac{\delta t}{2}\left[\left(\frac{F_f}{m} - \lambda_F^{(f)}\right)\frac{\partial}{\partial v} - \lambda_F^{(f)}\sum_{k=1}^L v_1^{(k)}\frac{\partial}{\partial v_1^{(k)}}\right]\right\}\right] \\
&\times \exp\left(\frac{\delta t}{2}v\frac{\partial}{\partial q}\right)\exp(iL_{OU}\delta t)\exp\left(\frac{\delta t}{2}v\frac{\partial}{\partial q}\right) \\
&\times \exp\left\{\frac{\delta t}{2}\left[\left(\frac{F_f}{m} - \lambda_F^{(f)}\right)\frac{\partial}{\partial v} - \lambda_F^{(f)}\sum_{k=1}^L v_1^{(k)}\frac{\partial}{\partial v_1^{(k)}}\right]\right\}^{n-2} \\
&\times \exp\left\{\frac{\delta t}{2}\left[\left(\frac{F_f}{m} - \lambda_F^{(f)}\right)\frac{\partial}{\partial v} - \lambda_F^{(f)}\sum_{k=1}^L v_1^{(k)}\frac{\partial}{\partial v_1^{(k)}}\right]\right\} \\
&\times \exp\left(\frac{\delta t}{2}v\frac{\partial}{\partial q}\right)\exp(iL_{OU}\delta t)\exp\left(\frac{\delta t}{2}v\frac{\partial}{\partial q}\right) \\
&\times \exp\left\{\frac{\delta t}{2}\left[\left(\frac{F_f + nF_s}{m} - (\lambda_F^{(f)} + n\lambda_F^{(s)})\right)\frac{\partial}{\partial v} - (\lambda_F^{(f)} + n\lambda_F^{(s)})\sum_{k=1}^L v_1^{(k)}\frac{\partial}{\partial v_1^{(k)}}\right]\right\} \\
&\times \exp\left(iL_N\frac{\Delta t}{2}\right) \tag{50}
\end{aligned}$$

The form of this factorization is largely formal in its construction. In practice, there is *no need* to split the evolution up into first, $n - 2$ intermediate, and last steps. Rather, in the first and last iterations of the RESPA loop, the force is taken to be $F_f + nF_s$ while for the remaining $n - 2$ iterations, it is simply F_f . Also, within this scheme, evolution produced

by the stochastic force term, which only affects $v_2^{(k)}$ can be derived using the Itô calculus and is given by

$$e^{iL_{\text{OU}}t}v_2^{(k)} = v_2^{(k)}(0)e^{-\gamma t} + \sigma R(t)\sqrt{\frac{1 - e^{-2\gamma t}}{2\gamma}} \quad (51)$$

where R is the random force at time t .

Note that in XO-RESPA, the purely extended system part involving iL_N is evaluated once at the beginning and once at the end of the step using a time step Δt . For XI-RESPA,

this operator is evaluated every small time step using the factorization:

$$\begin{aligned}
\exp(iL\Delta t) &= \exp\left(iL_N\frac{\delta t}{2}\right) \\
&\times \exp\left\{\frac{\delta t}{2}\left[\left(\frac{F_f+nF_s}{m}-\left(\lambda_F^{(f)}+n\lambda_F^{(s)}\right)\right)\frac{\partial}{\partial v}-\left(\lambda_F^{(f)}+n\lambda_F^{(s)}\right)\sum_{k=1}^Lv_1^{(k)}\frac{\partial}{\partial v_1^{(k)}}\right]\right\} \\
&\times \exp\left(\frac{\delta t}{2}v\frac{\partial}{\partial q}\right)\exp(iL_W\delta t)\exp\left(\frac{\delta t}{2}v\frac{\partial}{\partial q}\right) \\
&\times \exp\left\{\frac{\delta t}{2}\left[\left(\frac{F_f}{m}-\lambda_F^{(f)}\right)\frac{\partial}{\partial v}-\lambda_F^{(f)}\sum_{k=1}^Lv_1^{(k)}\frac{\partial}{\partial v_1^{(k)}}\right]\right\} \\
&\times \left[\exp\left(iL_N\frac{\delta t}{2}\right)\exp\left\{\frac{\delta t}{2}\left[\left(\frac{F_f}{m}-\lambda_F^{(f)}\right)\frac{\partial}{\partial v}-\lambda_F^{(f)}\sum_{k=1}^Lv_1^{(k)}\frac{\partial}{\partial v_1^{(k)}}\right]\right\}\right] \\
&\times \exp\left(\frac{\delta t}{2}v\frac{\partial}{\partial q}\right)\exp(iL_W\delta t)\exp\left(\frac{\delta t}{2}v\frac{\partial}{\partial q}\right) \\
&\times \exp\left\{\frac{\delta t}{2}\left[\left(\frac{F_f}{m}-\lambda_F^{(f)}\right)\frac{\partial}{\partial v}-\lambda_F^{(f)}\sum_{k=1}^Lv_1^{(k)}\frac{\partial}{\partial v_1^{(k)}}\right]\right\}\exp\left(iL_N\frac{\delta t}{2}\right)^{n-2} \\
&\times \exp\left\{\frac{\delta t}{2}\left[\left(\frac{F_f}{m}-\lambda_F^{(f)}\right)\frac{\partial}{\partial v}-\lambda_F^{(f)}\sum_{k=1}^Lv_1^{(k)}\frac{\partial}{\partial v_1^{(k)}}\right]\right\} \\
&\times \exp\left(\frac{\delta t}{2}v\frac{\partial}{\partial q}\right)\exp(iL_W\delta t)\exp\left(\frac{\delta t}{2}v\frac{\partial}{\partial q}\right) \\
&\times \exp\left\{\frac{\delta t}{2}\left[\left(\frac{F_f+nF_s}{m}-\left(\lambda_F^{(f)}+n\lambda_F^{(s)}\right)\right)\frac{\partial}{\partial v}-\left(\lambda_F^{(f)}+n\lambda_F^{(s)}\right)\sum_{k=1}^Lv_1^{(k)}\frac{\partial}{\partial v_1^{(k)}}\right]\right\} \\
&\times \exp\left(iL_N\frac{\delta t}{2}\right) \tag{52}
\end{aligned}$$

The action of $\exp(iL_{OUT})$ on the $v_2^{(k)}$ is shown in Eq. (51), and the action of the operator $\exp(tv\partial/\partial q)$ on q is a simple translation $q \rightarrow q+vt$. The action of the remaining operators is discussed below.

A. Solution for $\exp(iL_v t)$

The force appearing in the propagator $\exp(iL_v t)$ is either F_f or $F_f + nF_s$ depending on the step of the RESPA loop. As both F_f and F_s are both independent of v , we can simply solve the problem for a general F , which is either F_f or $F_f + nF_s$, depending on the operator that is being applied. For any general F , action of the operator $\exp(iL_v t)$ is equivalent to the solution of the differential equations

$$\dot{v} = \frac{F}{m} - \frac{v^2 F}{\Lambda}$$

$$\dot{v}_1^{(k)} = -\frac{v F}{\Lambda} v_1^{(k)} \quad (53)$$

where $\Lambda = L\beta^{-1}$. In these equations, F is treated as a constant, and the equations must be solved for an arbitrary initial condition $v(0)$, $v_1^{(k)}(0)$. These equations are nonlinear, however, an analytical solution is actually available for them. Following the procedure of Ref. 30, we write the differential equations in the form

$$\dot{v} = \frac{F}{m} - \dot{h}v$$

$$\dot{v}_1^{(k)} = -\dot{h}v_1^{(k)} \quad (54)$$

where $\dot{h} = v(t)F/\Lambda$. We then assume a solution of the form

$$v(t) = \frac{v(0) + (F/m)s(t)}{\dot{s}(t)}$$

$$v_1^{(k)}(t) = \frac{v_1^{(k)}(0)}{\dot{s}(t)} \quad (55)$$

where $s(t)$ is a function to be determined. Differentiating the ansatz for $v(t)$ with respect to time, we obtain

$$\dot{v} = \frac{F}{m} - \frac{\ddot{s}}{\dot{s}}v(t) \quad (56)$$

so that $\ddot{s}/\dot{s} = \dot{h}$. Given this relation, we see immediately that

$$\begin{aligned}\dot{s}(t) &= \exp \left[\int_0^t \dot{h}(t') dt' \right] = e^{h(t)} e^{-h(0)} \\ s(t) &= \int_0^t dt' e^{h(t')}\end{aligned}\tag{57}$$

so that $s(0) = 0$, and $\dot{s}(0) = 1$. The equation that $s(t)$ must satisfy is

$$\frac{\ddot{s}}{\dot{s}} = \dot{h} = \frac{F}{\Lambda} \left[\frac{v(0) + (F/m)s(t)}{\dot{s}} \right]\tag{58}$$

or

$$\ddot{s} - \frac{F^2}{m\Lambda} s - \frac{F}{\Lambda} v(0) = 0\tag{59}$$

This equation can be easily solved using Laplace transforms to yield

$$s(t) = \frac{1}{\sqrt{b}} \sinh(\sqrt{b}t) + \frac{a}{b} (\cosh(\sqrt{b}t) - 1)\tag{60}$$

where $a = Fv(0)/\Lambda$ and $b = F^2/m\Lambda$. With this and the corresponding expression for \dot{s}

$$\dot{s}(t) = \sinh(\sqrt{b}t) + \frac{a}{\sqrt{b}} \cosh(\sqrt{b}t)\tag{61}$$

Thus, the application of $\exp(iL_v \delta t/2)$ yields the following evolution step:

$$\begin{aligned}v\left(\frac{\delta t}{2}\right) &= \frac{v(0) + (F/m)s(\delta t/2)}{\dot{s}(\delta t/2)} \\ v_1^{(k)}\left(\frac{\delta t}{2}\right) &= \frac{v_1^{(k)}(0)}{\dot{s}(\delta t/2)}\end{aligned}\tag{62}$$

Note that if a and b are close to zero, the functions $s(t)$ and $\dot{s}(t)$ become 0/0 and should be evaluated as a power series in t . In practice, we have found that a fourth-order power series is sufficient when $\delta t \sqrt{b}/2 < 10^{-5}$.

B. Solution for $\exp(iL_N t)$

The operator $\exp(iL_N t)$ combines a Nosé-Hoover type evolution with a part of the isokinetic constraint. Thus, in order to solve this part of the problem, we first introduce a Suzuki-Yoshida factorization^{43–46} and write

$$e^{iL_N \tau/2} = \prod_{j=1}^{n_{sy}} \prod_{i=1}^{n_{res}} e^{iL_N w_j \tau/2n_{res}} \quad (63)$$

where $\tau = \Delta t$ or $\tau = \delta t$, depending on the choice of XO-RESPA or XI-RESPA. Here, w_j are the Suzuki-Yoshida weights, and n_{res} is associated with a second RESPA decomposition for this operator only and should not be confused with the RESPA decomposition being applied to the fast and slow forces. If, for example, $n_{sy} = 3$, then the weights are $w_1 = w_3 = 1/(2 - 2^{1/3})$, and $w_2 = 1 - w_1 - w_3$. Before we can proceed, we must further subdivide the operator $\exp(iL_N w_i \tau/2n_{res})$, as we cannot solve its full action explicitly. Thus, we write

$$iL_N = iL_{N,1} + iL_{N,2} \quad (64)$$

where

$$\begin{aligned} iL_{N,1} &= -\lambda_N v \frac{\partial}{\partial v} - \lambda_N \sum_{k=1}^L v_1^{(k)} \frac{\partial}{\partial v_1^{(k)}} - \sum_{k=1}^L v_2^{(k)} v_1^{(k)} \frac{\partial}{\partial v_1^{(k)}} \\ iL_{N,2} &= \sum_{k=1}^L \frac{G(v_1^{(k)})}{Q_2} \frac{\partial}{\partial v_2^{(k)}} \end{aligned} \quad (65)$$

and we write

$$e^{iL_N w_j \tau/2n_{res}} = e^{iL_{N,2} w_j \tau/4n_{res}} e^{iL_{N,1} w_j \tau/2n_{res}} e^{iL_{N,2} w_j \tau/4n_{res}} \quad (66)$$

The operator $\exp(iL_{N,2} w_j \tau/4n_{res})$ is just a simple translation operator.

The general evolution produced by the operator $\exp(iL_{N,1} \tau/2n_{res})$ is equivalent to the

solution of the differential equations

$$\begin{aligned} \dot{v} &= \frac{L}{(L+1)\Lambda} \left(\sum_{j=1}^L v_2^{(j)} \left(v_1^{(j)} \right)^2 \right) v \\ \dot{v}_1^{(k)} &= \frac{L}{(L+1)\Lambda} \left(\sum_{j=1}^L v_2^{(j)} \left(v_1^{(j)} \right)^2 \right) v_1^{(k)} - v_2^{(k)} v_1^{(k)} \end{aligned} \quad (67)$$

which are solved holding the $v_2^{(k)}$ fixed, and evaluation of the solution at $t = \tau/2n_{\text{res}}$. The equations must be solved for an arbitrary initial condition $v(0)$ and $v_1^{(k)}(0)$. Once again, although the equations are nonlinear, an analytical solution can be obtained by solving the equation for $v_1^{(k)}$ by direct separation, and then substituting the result into the equation for v . This procedure yields

$$\begin{aligned} v(t) &= v(0)H(t) \\ v_1^{(k)}(t) &= v_1^{(k)}(0)H(t)e^{-v_2^{(k)}t} \end{aligned} \quad (68)$$

where

$$H(t) = \sqrt{\frac{\Lambda}{mv^2(0) + \frac{L}{L+1} \sum_{j=1}^L Q_1 v_1^{(j)}(0)^2 e^{-2v_2^{(j)}t}}}} \quad (69)$$

Setting $t = \tau/2n_{\text{res}}$, these become

$$\begin{aligned} v\left(\frac{\tau}{2n_{\text{res}}}\right) &= v(0)H(\tau/2n_{\text{res}}) \\ v_1^{(k)}\left(\frac{\tau}{2n_{\text{res}}}\right) &= v_1^{(k)}(0)H(\tau/2n_{\text{res}})e^{-v_2^{(k)}\tau/2n_{\text{res}}} \\ H\left(\frac{\tau}{2n_{\text{res}}}\right) &= \sqrt{\frac{\Lambda}{mv^2(0) + \frac{L}{L+1} \sum_{j=1}^L Q_1 \left(v_1^{(j)} \right)^2 (0) e^{-2v_2^{(j)}\tau/2n_{\text{res}}}}} \end{aligned} \quad (70)$$

With the action of each operator specified, the entire MTS integrator is now explicit.

The stochastic-isokinetic Nosé-Hoover RESPA-based MTS integrator derived in this section is termed SIN(R) for short. Compared to the scheme of Ref. 26, the SIN(R) method is, despite appearances, considerably simpler to implement.

V. NUMERICAL EXAMPLES

In this section we provide numerical results which further inform the theoretical discussions of the previous sections. In the previous section, we described a numerical scheme, referred to as SIN(R), which is applicable to the general N -degree of freedom system and arbitrary L .

A. Weakly perturbed harmonic oscillator

A simple example illustrating the efficacy of the SIN(R) scheme is a harmonic oscillator of unit mass with an additional weak quartic perturbation, for which the potential is

$$U(q) = \frac{1}{2}\omega^2 q^2 + \frac{1}{4}gq^4 \quad (71)$$

The simple problem will serve to show that the most basic resonance phenomenon has been eliminated in the SIN(R) scheme just as it was in the original INR approach of Ref. 26. For this problem, the large or outer time step is set to the resonance time step π/ω . Figure 1 (left) shows the probability distribution $P(q)$ of the coordinate q for this problem when $\delta t = \Delta t/100$ and $L = 1$. The two distributions in this figure correspond to a standard Nosé-Hoover chain²⁷ RESPA calculation and one using SIN(R). Runs are of length $10^9 \Delta t$ and use $\gamma = 1$, $\omega = 3$, $g = 0.1$, $Q_1 = Q_2 = 1$, and $\beta = 1$. We also test

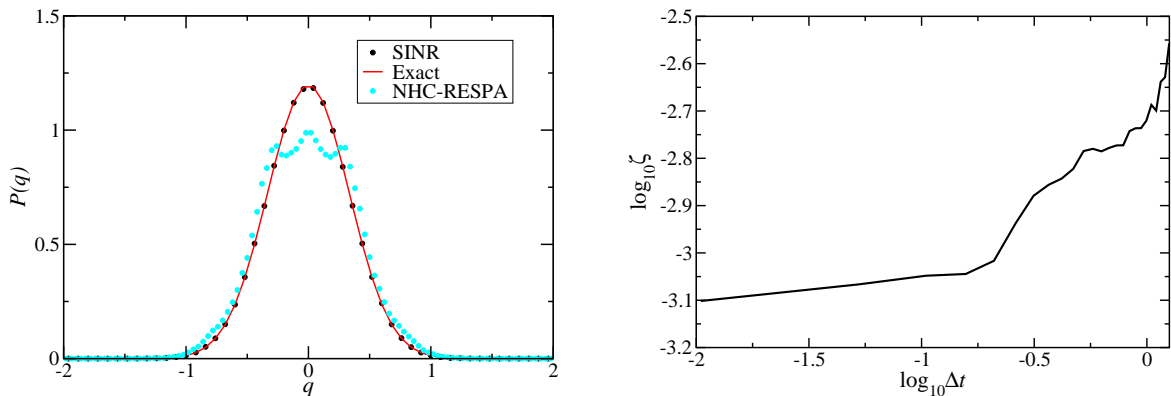


FIG. 1. (Left): Probability distribution $P(q)$ for the quartic potential in Eq. (71). Exact distribution (solid), SINR (black dots), Nosé-Hoover chain RESPA (cyan dots). (Right): Logarithm of the L^1 error vs. the logarithm of the large time step keeping the small time step fixed.

the sensitivity of the algorithm to the choices of the outer time step Δt by fixing δt and varying Δt in increments of 0.05 between $0.01\pi/\omega$ and $1.2\pi/\omega$ and plotting the L^1 error

$$\zeta = \frac{1}{N_b} \sum_{i=1}^{N_b} |P(q_i) - P_{\text{an}}(q_i)| \quad (72)$$

in Fig. 1. We see that the error is essentially monotonic over the entire range, suggesting that if any resonances exist (apart from the expected resonance at π/ω) in this interval, the method is not affected by them. We also test the sensitivity of the error to the values of Q_1 , Q_2 , and γ by plotting the L^1 error for different values of these parameters in Fig. 2. Here, N_b is the number of bins used to generate the distribution, q_i is the value of the coordinate in the i th bin, and $P_{\text{an}}(q)$ is the analytical distribution $P_{\text{an}}(q) \propto \exp(-\beta U(q))$. It can be seen that for a wide range of parameter values, the algorithm generates the same result with little change in the error, suggesting that within a reasonable range of values, the choice of parameters is not especially important.

B. A flexible water model

A challenging problem with a very wide separation of time scales is liquid water described by a fully flexible model⁴⁷. We first demonstrate the use of SIN(R) without RESPA in order to explore the sensitivity of the method as a thermostating approach to the choice of parameters. In Fig. 3, we show the oxygen-oxygen, oxygen-hydrogen, and hydrogen-hydrogen radial distribution functions for this model for different values of γ in a system of 512 molecules in a box of length 25 Å subject to periodic boundary conditions. In these simulations, the time step is 0.5 fs, and $Q_1 = Q_2 = k_B T \tau^2$ where T is the temperature of the simulation, i.e., 300 K, $\tau = 10$ fs, and $L = 4$. Electrostatic interactions are treated using the smooth particle-mesh Ewald method (SPME)⁴⁸. The SIN(R) RDFs are shown compared to a benchmark set of RDFs generated in the NVT ensemble using a Nosé-Hoover chain (NHC) thermostat²⁷. on each degree of freedom and a time step of 0.5 fs. Simulation lengths range between 300 and 600 ps and are run using the PINY_MD code⁴⁹. It can be seen from the figure that the results are not sensitive to the value of the friction parameter in the chosen range. As a further test of robust against the parameter

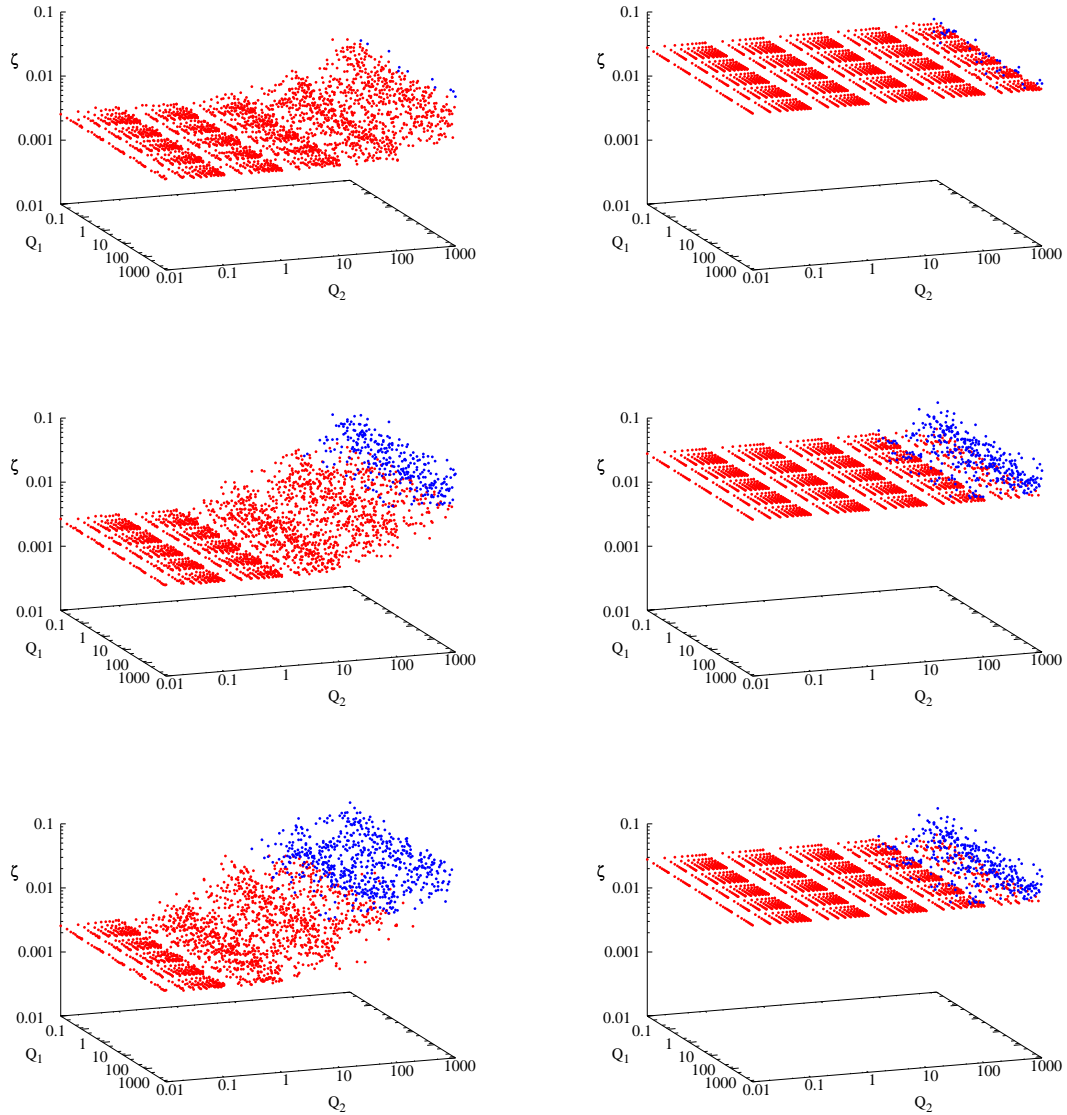


FIG. 2. L^1 error (see Eq. (72) of the position distribution $P(q)$ for the quartic potential in Eq. (71) for different values of the parameters Q_1 , Q_2 , γ , and the number of RESPA steps. Top: $\gamma = 0.1$ with 10 RESPA steps (left) and 100 RESPA steps (right). Middle: $\gamma = 1.0$ with 10 RESPA steps (left) and 100 RESPA steps (right). Bottom: $\gamma = 10.0$ with 10 RESPA steps (left) and 100 RESPA steps (right). Red and blue dots separate values of ζ into two regions: For 10 RESPA steps, $\zeta < 0.02$ is designated with red dots, $\zeta > 0.02$ is designated with blue dots. For 100 RESPA steps, the dividing value is $\zeta = 0.03$.

choice, we show the L^1 error of the three radial distribution functions relative to NVT benchmark. These are shown in Fig. 4. It can be seen that for a wide range of values of Q_1 and Q_2 the error is small and not particularly sensitive to specific values of these

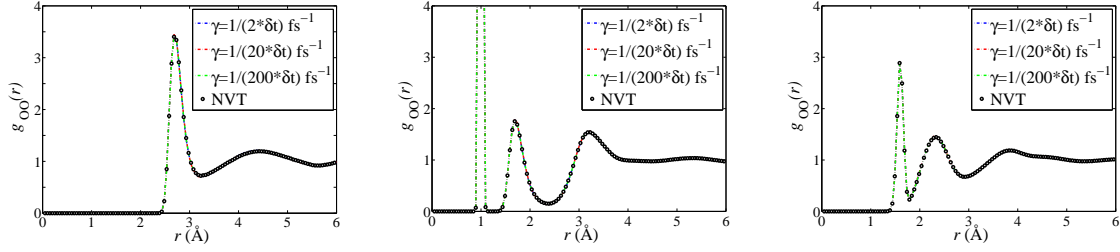


FIG. 3. Oxygen-oxygen (left), oxygen-hydrogen (middle) and hydrogen-hydrogen (right) radial distribution functions for γ values of $0.5/\delta t$, $0.05/\delta t$, and $0.005/\delta t$, where $\delta t = 0.5$ fs.

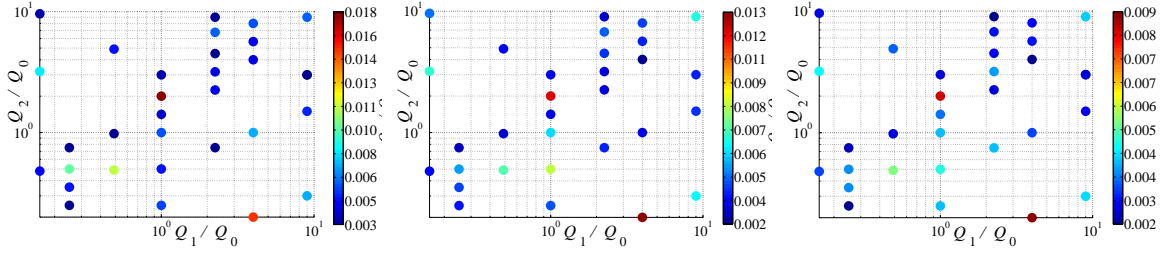


FIG. 4. L^1 error in the three RDFs for different values of Q_1 and Q_2 . In these simulations, $\gamma = 0.05/\delta t$, where $\delta t = 0.5$ fs.

parameters. Not unexpectedly, however, as Q_2 increases, the error does as well, since in this limit, the stochastic kicks have a smaller influence, and convergence becomes slower.

Because of resonance, MTS methods for flexible water have not been able to achieve outer time steps larger than about 5 fs^{24,25}. Here, we divide the forces into three time scales corresponding to intramolecular motion (bond and bend vibrations), short-range intermolecular interactions, which include all non-bonded interactions within a cutoff r_{sr} , and long-range interactions. For the latter, we consider two types: First, we consider the scheme suggested in Refs. 23 and 50, in which the long-range potential is expressed using Ewald summation for the electrostatic interaction, and is given by

$$\begin{aligned}
 U_{\text{long}}^{(2)}(\mathbf{r}) = & U_{\text{recip}}(\mathbf{r}; \alpha, k_{\text{max}}) \\
 & - \sum_{\mathbf{S}} \sum_i \sum_{j \geq i} \left(1 - \delta_{ij}^{(0)}\right) (1 - \theta(r_{ij,\mathbf{S}} - r_{\text{cut}})) q_i q_j \frac{\text{erf}(\alpha r_{ij,\mathbf{S}})}{r_{ij,\mathbf{S}}} \quad (73)
 \end{aligned}$$

where the sum over \mathbf{S} is a sum over all periodic images, $r_{ij,\mathbf{S}} = |\mathbf{r}_i - \mathbf{r}_j + \mathbf{S}|$, $\delta_{ij}^{(0)} = 1$ only if $i = j$ and $\mathbf{S} = (0, 0, 0)$, $\theta(x)$ is the Heaviside step function, q_i is the charge on atom

i , $\text{erf}(x)$ is the error function, $U_{\text{recip}}(\mathbf{r})$ is the reciprocal-space contribution to the Ewald sum for electrostatic interactions, the parameter α determines the range of the real-space part of the Ewald sum, k_{max} is the maximum magnitude of the reciprocal-space lattice vectors used to evaluate the long-range part of the electrostatic interaction. We refer to this subdivision as RESPA2. The second choice divides both the real and reciprocal space sums into short and long-range contributions. The long range term then becomes

$$U_{\text{long}}^{(1)}(\mathbf{r}) = U_{\text{recip}}(\mathbf{r}; \alpha, k_{\text{res}}) + \sum_{\mathbf{S}} \sum_i \sum_{j \geq i} \left(1 - \delta_{ij}^{(0)}\right) \theta(r_{ij,\mathbf{S}} - r_{\text{cut}}) q_i q_j \frac{\text{erf}(\alpha r_{ij,\mathbf{S}})}{r_{ij,\mathbf{S}}} \quad (74)$$

where $k_{\text{res}} < k_{\text{max}}$ is a reciprocal-space cutoff that picks out reciprocal-space vectors with small magnitudes, corresponding to the long-range contributions. We refer to this subdivision as RESPA1. Eq. (74) might offer some advantages over Eq. (73) in that it does not rely on a potentially imperfect cancellation between real- and reciprocal-space short-range contributions, which can cause numerical issues in Ewald summation in flexible systems⁵¹.

In the present simulations, SIN(R) is used with time steps of $\delta t = 0.5$ fs for the intramolecular interactions, $\Delta t = 3.0$ fs for the short-range interactions, and the outermost time step ΔT is allowed to vary in order to see how large it can be chosen without degrading physical observables. In all simulations, we choose the values of the Q_1 and Q_2 using a value of $\tau = 10$ fs.

In Fig. 5, we show radial distribution functions (RDFs) corresponding to the RESPA1 scheme for outer time steps $\Delta T = 9$ fs, 60 fs, and 99 fs using $L = 4$, which allows us to test robustness of SIN(R) with this parameter. In addition, we employ a friction $\gamma = 0.1$ fs⁻¹ and the XI-RESPA scheme. Dependence on L and the choice of XO-RESPA vs. XI-RESPA will be tested below. In these calculations, the short-range cutoff is 6.0 Å, and the SPME reciprocal-space cutoff for the long-range interaction is half that used for the full reciprocal-space cutoff. The RDFs in Fig. 5 are of comparable accuracy to those in Ref. 26 even at a time step of 99 fs. The SIN(R) RDFs are compared to those generated from a benchmark simulation in the canonical ensemble using a single time step of 0.5 fs.

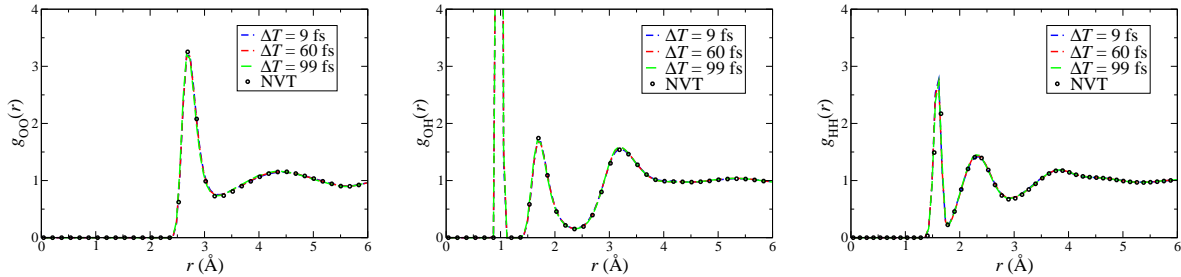


FIG. 5. Oxygen-oxygen (left), oxygen-hydrogen (middle) and hydrogen-hydrogen (right) radial distribution functions generated by SIN(R) for the RESPA1 scheme of Eq. (74) with different choices for the outer time step ΔT : 9 fs (blue), 60 fs (red), 99 fs (green). The benchmark NVT result is shown as black circles.

In Fig. 6, we plot the L^1 error for each simulation relative to its final, converged value.

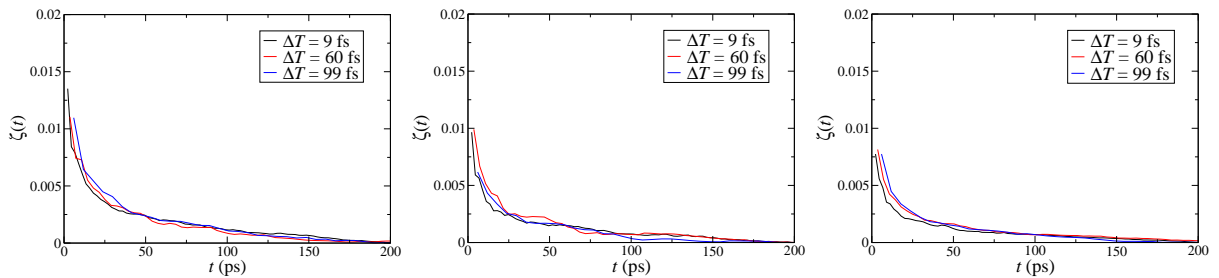


FIG. 6. L^1 error $\zeta(t)$ relative to the fully converged value for each SIN(R) simulation shown in Fig. 5. $\Delta T = 9$ fs (black), $\Delta T = 60$ fs (red), $\Delta T = 99$ fs (blue).

The purpose of this comparison is to test whether the increase in the outer time step ΔT and varying friction leads to a change in the rate of convergence. According to Fig. 6, the convergence rates of all three simulations are similar, suggesting the different choices of outer time step, friction, and value of L do not strongly affect the convergence rate.

The RDFs for RESPA2 are shown in Fig. 7, here using outer time steps of $\Delta T = 6$ fs, 60 fs, and 99 fs. It is important to note that the RESPA2 scheme is somewhat sensitive to the choice of the short-range cutoff length, which we take to be 8 \AA in the present simulations. The RESPA2 scheme also requires a smooth switch to be applied to the forces²², and the stability of the scheme is sensitive to the order of the switch. Here, we employ a quintic switching function. The corresponding L^1 error plots are shown in Fig. 8. As these are somewhat more featured than the L^1 error plots of Fig. 6, we extend the time axis somewhat compared to that of Fig. 6. Fig. 8 again show that the rate of convergence

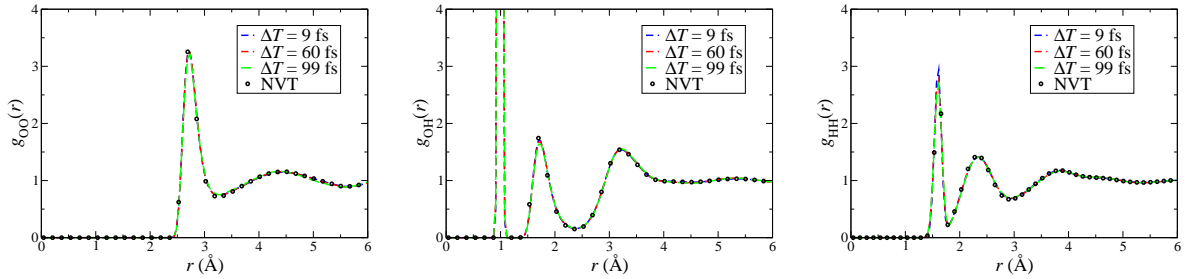


FIG. 7. Oxygen-oxygen (left), oxygen-hydrogen (middle) and hydrogen-hydrogen (right) radial distribution functions generated by SIN(R) for the RESPA2 scheme of Eq. (73) with different choices for the outer time step ΔT : 6 fs (blue), 60 fs (red), 99 fs (green). The benchmark NVT result is shown as black circles. As in the RESPA1 example, all simulations employ a value of $L = 4$.

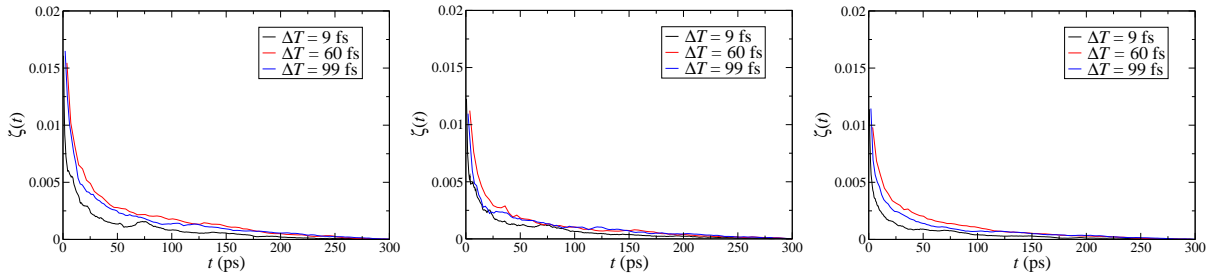


FIG. 8. L^1 error $\zeta(t)$ relative to the fully converged value for each SIN(R) simulation shown in Fig. 7. $\Delta T = 9$ fs (black), $\Delta T = 60$ fs (red), $\Delta T = 99$ fs (blue).

is not strongly affected by the length of the outer time step, provided the parameters are carefully chosen²². Interestingly, in our implementation, the computational overhead of RESPA1 with its shorter short-range cutoff and incorporation of reciprocal space into the short-range reference system is similar to that of RESPA2 with a purely real-space short-range reference system and larger short-range cutoff. Clearly, however, implementation details will influence this balance, and the use of massively parallel FFTs or GPUs for real-space force calculations could reduce the overhead of the reference system, thereby improving the efficiency of r-RESPA integration schemes.

We next examine the dependence on the choice of L by showing the RDFs for RESPA1 and RESPA2 with $L = 1$, $L = 2$, and $L = 4$ in Fig. 9. In these simulations $\Delta T = 60$ fs, and $\gamma = 0.1$ fs⁻¹. The L^1 error plot in the right panel corresponds to the RESPA1 case and illustrates that convergence is also insensitive to the choice of L .

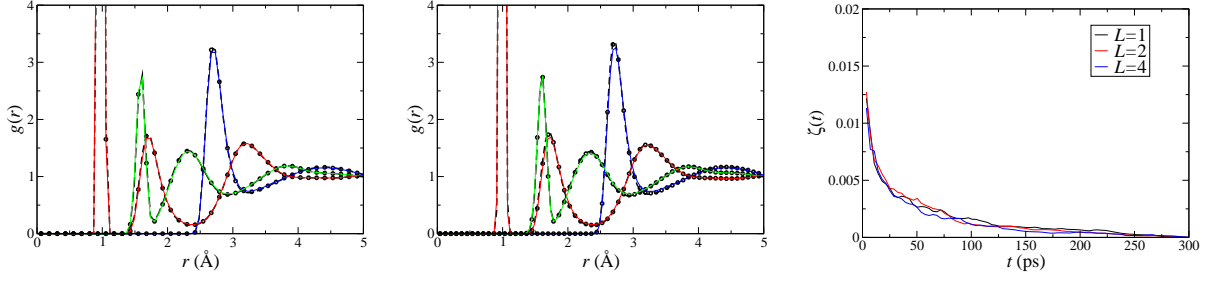


FIG. 9. Complete set of radial distribution functions for RESPA1 (left) and RESPA2 (middle) for $L = 1$, $L = 2$, and $L = 4$. The $L = 4$ RDFs are shown as blue (oxygen-oxygen), red (oxygen-hydrogen), and green (hydrogen-hydrogen) solid lines. $L = 1$ is shown with the dashed line, and $L = 2$ is shown as circular symbols. In the right panel, we show the L^1 error for the oxygen-oxygen RDF for the RESPA1 scheme.

Finally, we show that both XI-RESPA and XO-RESPA are capable of reproducing the RDFs. This is illustrated in Fig. 10, which displays RDFs generated XO-RESPA1 and XO-RESPA2 and comparing these to the NVT benchmark results. For these simulations,

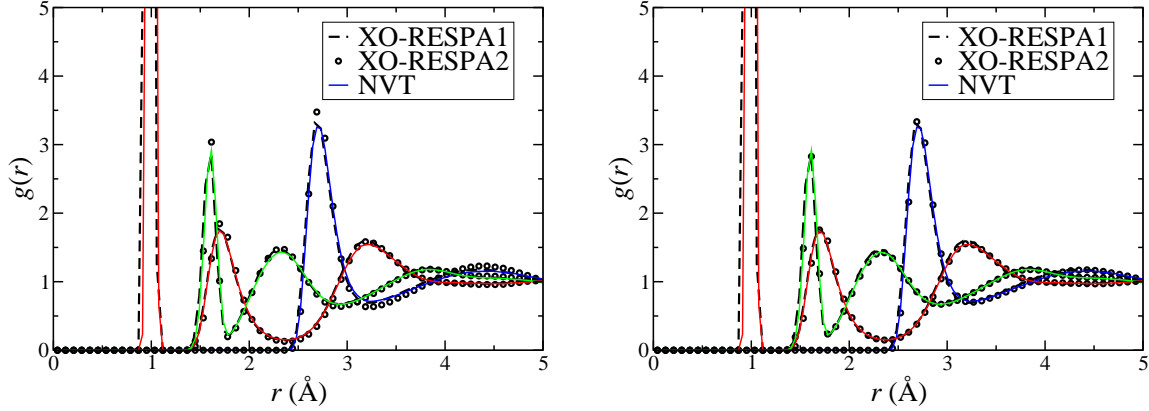


FIG. 10. RDFs generated using XO-RESPA1 (dashed line) and XO-RESPA2 (symbols), compared to the NVT benchmark (colored solid lines – oxygen-oxygen(blue), oxygen-hydrogen (red), hydrogen-hydrogen (green)). **Left:** $\Delta T = 60$ fs for XO-RESPA2; **Right:** $\Delta T = 30$ fs for XO-RESPA2.

$L = 4$, $\gamma = 0.1 \text{ fs}^{-1}$, and $\Delta T = 60$ fs. Here, we can see that, while both are in reasonable agreement with the NVT benchmark, the RESPA2 results show a slightly larger deviation than the corresponding XI-RESPA2 RDFs, illustrating that this scheme is somewhat more sensitive to the choice of the simulation parameters, as alluded to previously. We have also run this case with an outer time step of $\Delta T = 30$ fs and have found that the deviations

in Fig. 10 largely disappear (see Fig. 10).

VI. CONCLUSIONS

We have introduced a stochastic resonant-free multiple time step approach for molecular dynamics calculations involving forces that drive motion on many time scales. The method builds on the previous work of Minary *et al.*²⁶ and is shown to allow very large time steps to be employed for the slowest forces, similar to what was obtained previously²⁶. The new stochastic version of the algorithm, termed SIN(R), both simplifies the implementation of the method and can be shown to be ergodic. We presented the details of a multiple time step algorithm for the equations of motion and demonstrated the performance on both a simple, illustrative problem and a more realistic flexible water model. It was shown that time steps as large as 100 fs could be employed for the long-range forces in a flexible water model. The results display a slight sensitivity to the choice of force subdivision, indicating that when very large time steps are used some care must be exercised in choosing how short and long range intermolecular forces are defined. We have demonstrated the performance of the approach for a typical fixed-charge model. However, we also expect the present approach to be useful in simulation of complex systems employing polarizable models and could even enhance the efficiency of *ab initio* molecular dynamics calculations. Investigations into the possible utility of the present approach in calculations of this type will be the subject of future research.

ACKNOWLEDGMENTS

The authors gratefully acknowledge useful discussions with Dr. Joseph A. Morrone. M.E.T. and D. T. M. acknowledge support from NSF CHE-1012545 and CHE-1301314. B.J.L acknowledges the support of the CWI (Amsterdam) and an NWO (Netherlands) “visitors grant” as well as useful conversations with A. Davie.

REFERENCES

- ¹T. HUBER, A. E. TORDA, and W. F. VAN GUNSTEREN, *J. Comput.-Aided Mol. Des.* **8**, 695 (1994).
- ²H. GRUBMÜLLER, *Phys. Rev. E* **52**, 2893 (1995).
- ³E. DARVE and A. POHORILLE, *J. Chem. Phys.* **115**, 9169 (2001).
- ⁴L. ROSSO and M. E. TUCKERMAN, *Molec. Sim.* **28**, 925 (2002).
- ⁵L. ROSSO, P. MINARY, Z. ZHU, and M. E. TUCKERMAN, *J. Chem. Phys.* **116**, 4389 (2002).
- ⁶L. ROSSO, J. B. ABRAMS, and M. E. TUCKERMAN, *J. Phys. Chem. B* **109**, 4162 (2005).
- ⁷A. LAIO and M. PARRINELLO, *Proc. Natl. Acad. Sci.* **99**, 12562 (2002).
- ⁸J. HÉNIN and C. CHIPOT, *J. Chem. Phys.* **121**, 2904 (2004).
- ⁹P. MINARY, M. E. TUCKERMAN, and G. J. MARTYNA, *SIAM J. Sci. Comput.* **30**, 2055 (2007).
- ¹⁰E. DARVE, D. RODRÍGUEZ-GÓMEZ, and A. POHORILLE, *J. Chem. Phys.* **128**, 144120 (2008).
- ¹¹L. MARAGLIANO and E. VANDEN-EIJNDEN, *Chem. Phys. Lett.* **426**, 168 (2006).
- ¹²J. B. ABRAMS and M. E. TUCKERMAN, *J. Phys. Chem. B* **112**, 15742 (2008).
- ¹³B. DICKSON, F. LEGOLL, T. LELIEVRE, G. STOLTZ, and P. FLEURAT-LESSARD, *J. Phys. Chem. B* **114**, 5823 (2010).
- ¹⁴T. Q. YU and M. E. TUCKERMAN, *Phys. Rev. Lett.* **107**, 015701 (2011).
- ¹⁵M. CHEN, M. CUENDET, and M. E. TUCKERMAN, *J. Chem. Phys.* **137**, 024102 (2012).
- ¹⁶M. TUCKERMAN, B. J. BERNE, and G. J. MARTYNA, *J. Chem. Phys.* **97**, 1990 (1992).
- ¹⁷R. ZHOU and B. J. BERNE, *J. Chem. Phys.* **103**, 9444 (1995).
- ¹⁸S. J. STUART, R. ZHOU, and B. J. BERNE, *J. Chem. Phys.* **105**, 1426 (1996).
- ¹⁹G. J. MARTYNA, M. E. TUCKERMAN, D. J. TOBIAS, and M. L. KLEIN, *Mol. Phys.* **87**, 1117 (1996).
- ²⁰F. FIGUEIRIDO, R. M. LEVY, R. ZHOU, and B. J. BERNE, *J. Chem. Phys.* **106**, 1426 (1997).
- ²¹I. P. OMELYAN, *J. Chem. Phys.* **131**, 104101 (2009).

- ²²J. A. MORRONE, R. ZHOU, and B. J. BERNE, *J. Chem. Theor. Comput.* **6**, 2010 (1798).
- ²³J. A. MORRONE, T. E. MARKLAND, R. ZHOU, M. CERIOTTI, and B. J. BERNE, *J. Chem. Phys.* **134**, 2011 (014103).
- ²⁴T. SCHLICK, M. MANDZUIK, R. D. SKEEL, and K. SRINIVAS, *J. Comput. Phys.* **140**, 1 (1998).
- ²⁵Q. MA, J. A. IZAGUIRRE, and R. D. SKEEL, *SIAM J. Sci. Comput.* **24**, 1951 (2003).
- ²⁶P. MINARY, M. E. TUCKERMAN, and G. J. MARTYNA, *Phys. Rev. Lett.* **93**, 150201 (2004).
- ²⁷G. J. MARTYNA, M. L. KLEIN, and M. TUCKERMAN, *J. Chem. Phys.* **97**, 2635 (1992).
- ²⁸D. J. EVANS and G. P. MORRISS, *Statistical Mechanics of Nonequilibrium Liquids*, Harcourt Brace Javanovich, London, 1980.
- ²⁹F. ZHANG, *J. Chem. Phys.* **106**, 6102 (1997).
- ³⁰P. MINARY, G. J. MARTYNA, and M. E. TUCKERMAN, *J. Chem. Phys.* **118**, 2510 (2003).
- ³¹M. E. TUCKERMAN, *Statistical Mechanics: Theory and Molecular Simulation*, Oxford University Press, Oxford, 2010.
- ³²I. P. OMELIAN and A. KOVALENKO, *J. Chem. Phys.* **135**, 234107 (2011).
- ³³M. E. TUCKERMAN, C. J. MUNDY, and G. J. MARTYNA, *Europhys. Lett.* **45**, 149 (1999).
- ³⁴M. E. TUCKERMAN, Y. LIU, G. CICCOTTI, and G. J. MARTYNA, *J. Chem. Phys.* **115**, 1678 (2001).
- ³⁵A. A. SAMOLETOV, C. P. DETTMANN, and M. A. J. CHAPLAIN, *Journal of Statistical Physics* **128**, 1321 (2007).
- ³⁶B. LEIMKUHNER, F. NOORIZADEH, and F. THEIL, *J. Stat. Phys.* **135**, 261 (2009).
- ³⁷S. P. MEYN and R. L. TWEEDIE, *Markov chains and stochastic stability (2nd edition)*, Cambridge University Press, 2009.
- ³⁸L. REY-BELLET, Ergodic Properties of Markov Processes, in *Open Quantum Systems II*, edited by S. ATTAL, A. JOYE, and C.-A. PILLET, volume 1881 of *Lecture Notes in Mathematics*, pp. 1–39, Springer, Berlin, 2006.

- ³⁹M. HAIRER, Convergence of Markov Processes, Lecture notes, University of Warwick, 2010.
- ⁴⁰J. C. MATTINGLY, A. M. STUART, and D. J. HIGHAM, *Stoch. Proc. Appl.* **101**, 185 (2002).
- ⁴¹L. C. G. ROGERS and D. WILLIAMS, *Diffusions, Markov Processes, and Martingales, Vol.2: Itô Calculus*, John Wiley & Sons, 1987.
- ⁴²B. LEIMKUHNER and C. MATTHEWS, *Appl. Math. Res. Express* **2013**, 34 (2013).
- ⁴³M. SUZUKI, *J. Math. Phys.* **32**, 400 (1991).
- ⁴⁴H. YOSHIDA, *Phys. Lett. A* **150**, 262 (1990).
- ⁴⁵M. SUZUKI, *J. Math. Phys.* **32**, 400 (1991).
- ⁴⁶M. SUZUKI, *J. Phys. Soc. Japan* **61**, 3015 (1992).
- ⁴⁷F. PAESANI, W. ZHANG, D. A. CASE, T. E. CHEATHAM, and G. A. VOTH, *J. Chem. Phys.* **125**, 184507 (2006).
- ⁴⁸U. ESSMANN, L. PERRERA, M. BERKOWITZ, T. DARDEN, H. LEE, and L. G. PEDERSEN, *J. Chem. Phys.* **103**, 8577 (1995).
- ⁴⁹M. TUCKERMAN, D. YARNE, S. SAMUELSON, A. HUGHES, and G. MARTYNA, *Comp. Phys. Comm.* **128**, 333 ((2000)).
- ⁵⁰S. J. STUART, R. H. ZHOU, and B. J. BERNE, *J. Chem. Phys.* **105**, 1996 (1426–1436).
- ⁵¹P. PROCACCI, M. MARCHI, and G. J. MARTYNA, *J. Chem. Phys.* **108**, 1998 (8799–8803).